

Parameter Modeling for Small-Scale Mobility in Indoor THz Communication

Rohit Singh¹, Douglas Sicker^{1,2}

¹ *Engineering & Public Policy, Carnegie Mellon University, Pittsburgh, USA*

² *School of Computer Science, Carnegie Mellon University, Pittsburgh, USA*

Email: rohits1@andrew.cmu.edu, sicker@cmu.edu

ABSTRACT

Despite such challenges as high path loss and equipment cost, THz communication is becoming one of the potentially viable means through which ultra-high data rate can be achieved. To compensate for the high path loss, we present parameter modeling for indoor THz communication. To maximize efficient and opportunistic use of resources, we analyze the potential workarounds for a single access point to satisfy most of the mobile terminals by varying such parameters as humidity, distance, frequency windows, beamwidths, antenna placement, and user mobility type. One promising parameter is antenna beamwidth, where narrower beams results in higher antenna gain. However, this can lead to “*beamwidth dilemma*” scenario, where narrower beamwidth can result in significant outages due to device mobility and orientation. In this paper, we address this challenge by presenting a mobility model that performs an extensive analysis of different human mobility scenarios, where each scenario has different data rate demands and movement patterns. We observe that for mobile users, there are optimal beamwidths that are affected by the mobility type (high mobility, constrained mobility, and low mobility) and AP placement.

KEYWORDS

Terahertz, Indoor Model, Adaptive Frequency Window, Antenna Beamwidth, Beamwidth Dilemma, AP Placement.

I. INTRODUCTION

In the near future, the current 4G, WiFi systems, and even 5G systems will not be able to meet the anticipated demand for higher throughput and Quality of Service (QoS) [1]. Even with the best signal-to-interference-noise ratio (SINR), there is a theoretical limit to the achievable data rate, which is directly proportional to the available bandwidth. Obtaining additional bandwidth is one of the primary ways to achieve higher throughput. The mmWave (10 – 300GHz) bands are already being explored as a means to achieve a system average of 3–7Gbps data rate [2]. The next-generation IEEE 802.11ay is focused explicitly on catering to applications, such as VR

and AR games [3]. A more promising solution is to move to terahertz (THz) band (300GHz – 10THz) that can help provide higher throughput, in myriad number of applications including recreational indoor applications (e.g., gaming), educational purposes in schools, business communications, hologram communication, 8KTV, hospital patient monitoring, and public safety communications [5].

One of the biggest challenges of THz band is the high path loss, a combination of high absorption loss due to water vapor concentration (shown in Fig. 1a and 1b [4]) and high spreading loss directly proportional to the square of frequency and distance (shown in Fig. 1c and 1d). Thus, the total path loss is generally greater than 100dB, with occasional peaks approaching more than 200dB. Current research is focused on tackling this challenge by implementing better channel model [7], modulation schemes [6], beam alignment strategy [8] and antenna subarray structure [9]. Many researchers have tried to compensate for this high path loss by increasing the transmit power or antenna gain. The current THz antennas are limited to a transmit power of 0dBm and increasing it to 10dBm for frequency beyond 300GHz is still a challenge [10]. Antenna gain can be improved by using more directional antenna & narrow beamwidth [9] to improve the received signal. Typical beamwidths range from 1° to 20°, with a result of 47dBi to 21dBi gain. Although THz access-points are likely to be deployed in an indoor setting, small fluctuation for indoor devices mounted on body, hand, or head movement can still cause momentary outages, eventually resulting in lower average throughput [11].

Given that THz beams are so sensitive to user mobility, the location of AP becomes critical for efficient resource utilization. For a single user mode, the AP can be placed as close to the user equipment (UE) as possible with a direct line-of-sight (LOS). However, if we want to cover multiple UEs, the antenna has to be provided with the best degree of freedom (DoF), which is likely available only from the ceiling of the room. Nevertheless, having multiple APs will increase the chances of higher throughput and reduced outages. However, in many scenarios, it might not be possible to use these resources efficiently. Thus, it is worthwhile to consider efficient antenna resource allocation in THz bands.

In this paper, we evaluate the optimal system and mobility parameters required for higher throughput and user coverage for both static and mobile indoor THz devices. As we

This project was funded by CMU Portugal Program: CMU/TMP/0013/2017- THz Communication for Beyond 5G Ultra-fast Networks. We acknowledge Dr. Kazi Mohammed Saidul Huq (from Instituto de Telecomunicaes, Portugal) in his early work in discussing this concept with the authors

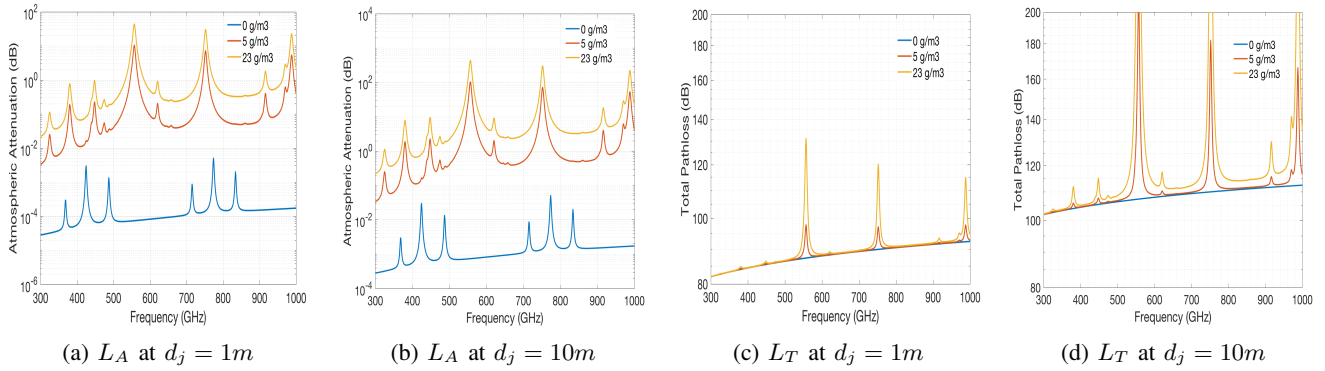


Fig. 1: Atmospheric loss L_A & Total Path loss L_T for different concentration of water vapor at 25°C for 1m and 10m distance

move to THz, managing and monitoring parameters, such as distance, humidity, frequency, bandwidth, antenna properties, and user mobility type, becomes critical for system efficiency. Some of these parameters are either dependent on technology advancements or environmental conditions and cannot be adjusted. However, we can still adjust the antenna properties dynamically by the devices to maintain system efficiency. For example, in THz the need for narrow beams makes it necessary that the beamwidth is selected wisely since it can lead to the “*beamwidth dilemma*”- narrower beamwidth means better gain and higher throughput, but with frequent outages due to rapid mobility and orientation of the device can eventually reduce the average throughput. We identify the system and mobility level changes required for THz communication and highlight the solutions using simulation by introducing different types of system impairments to illustrate ways of achieving the best system performance. We have also analyzed schemes through which THz resources can be used to economically and opportunistically to answer the following research questions: (i) what are the small-scale mobility-induced outage scenarios in THz, (ii) what are the mobility parameters through which we can monitor these mobility induced outages, (iii) what is the optimal antenna beamwidth for different parameters, and (iv) how many users can a single THz-AP satisfied economically in a multi-user model.

The rest of the paper is organized as follows. In Section II, we discuss the system parameter interdependencies and the tradeoffs required for a static model. In Section III, we characterize different human actions using a set of mobility parameters to identifying the mobility induced outage scenarios. In Section IV, we introduce environment settings to evaluate the mobility model and discuss the impact of the choice of beamwidth and antenna placement on throughput and user coverage, followed by a conclusion in Section V.

II. A STATIC MODEL

Setting aside mobility, we analyze users on a snapshot basis to explore the parameter adjustments available at the system level that can be optimized to increase throughput. The analysis done in this section will not only aid in our mobility model, but also for applications that are static in nature, such as 8K TV, hologram communication, short-haul

point to point communication, or even high-speed backhaul fiber replacement.

Fig. 1 shows that due to high path loss coupled with occasional attenuation peaks there are optimal frequency windows for THz devices to operate. These operating frequencies are mostly dependent on the distance d_j for a user j and water vapor concentration ρ . However, these factors are uncertain and dependent on the environment. Therefore, we build a static model that can adaptively select frequency windows based on distance and humidity. To do so we first need to quantify the relationship between frequency and other system parameters.

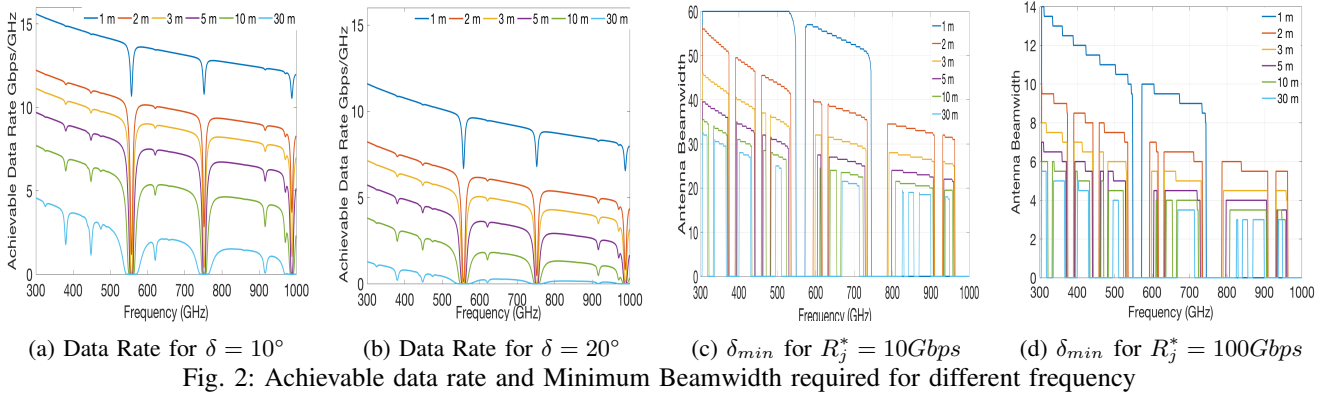
To compensate for the huge path-losses, using more directional antennas with narrow beams can help improve the signal strength. While directional THz antennae have irregular main lobes and side lobes, for simplicity, in this paper we assume an antenna pattern with perfect conical shaped main lobe (and we recognize the implication of this assumption). For a perfect main lobe, the antenna gain G can be represented as $G = \frac{X}{\delta_h \delta_v}$, where δ_h and δ_v are horizontal and vertical beamwidths in degrees, and X is an aperture dependent factor, which is equal to 52, 525 for a uniformly illuminated circular aperture [14] and 41, 253 for uniformly illuminated rectangular aperture [14]. We assume that the vertical and the horizontal beams are equal, i.e., $\delta_h = \delta_v = \delta$; thus, the new antenna gain is $G = \frac{X}{\delta^2}$, which is similar to the one proposed in [11].

Based on the antenna gain, we can calculate the achievable capacity R_j at specific center frequencies f_c . We can calculate R_j using Equation 2 [13], where B_j is the bandwidth, P_t is the transmit power, G_t and G_r are gains at transmitter and receiver respectively, $L_T(f_c, d_j, \rho)$ is the total path loss and N_o the noise power spectral density in dB/Hz .¹

$$R_j = B_j \log\left(1 + \frac{P_t * G_t(\delta) * G_r(\delta)}{L_T(f_c, d_j, \rho) * N_o}\right) \quad (1)$$

Based on Equation 2, we observe that the achievable data rate is mostly dependent on bandwidth B_j , center frequency f_c , separation d_j and beamwidth δ . A comparison of these parameters are shown in Figs. 2a and 2b. It seems that the beamwidth only scales up the data rate and is not affecting the huge data rate dips. These sudden data rate dips become

¹ We assume a noise power of $-193.85\text{dB}/\text{Hz}$, which can be calculated as $N_o = 10\log_{10}(N_f K T_k)$, where N_f is the noise figure of 10dB , K is the Boltzmann constant of $1.3810e^{-23}$, and T_k is the temperature in Kelvin.



prominent as we increase the separation d_j . Thus, for higher Eucladian distance d_j , the continuous frequency bands decrease, resulting in decrease in additional bandwidth.

To obtain higher throughput, it is necessary that we have continuous “frequency-windows” with wider bandwidths. These discontinuities on the frequency domain can be estimated using d_j for a particular user and clipping of the frequency bands with huge data rate dips. For a constant ρ of $5g/m^3$ at room temperature of $25^\circ C$, we assume that an AP can either adaptively select a frequency-window or use a pre-calculated lookup table for optimal throughput. A sample frequency-window lookup table for varying distances is shown in Table I. As we keep on increasing the distance d_j , the number of windows increase and the window size (or bandwidth) decreases. It is interesting to observe that at a distance of $30cm$ we can almost avail an uninterrupted bandwidth $250GHz$, and at $10m$ we can hardly get $50GHz$ of bandwidth. For the rest of the paper, we assume that each user can select the best frequency-window adaptively based on the environmental parameters.

Based on the analysis shown in Table I, we can estimate a relationship between the minimum beamwidth and center frequency required for a static user. For a given distance and water concentration, a theoretical bound for the minimum antenna beamwidths δ_{min} required by a center frequency f_c and bandwidth B_j is shown in Equation 2, which is specific to a particular antenna aperture X as explained in earlier. After clipping off the data rate dips and using Equation 2, we can have a plot for the minimum beamwidth required for particular f_c and d_j , as shown in Fig. 2c and 2d, for $B_j = 10GHz$ and $X = 52525$. As the requested data rate increases from $10Gbps$ to $100Gbps$ the δ_{min} values decreases rapidly.

$$\delta_{min} = \left[\frac{X^2 * P_t}{L_T(f_c, d_j, \rho) * N_o * (2^{R_j^*/B_j} - 1)} \right]^{1/4} \quad (2)$$

TABLE I: A frequency-window lookup table for varying distances

Distance	Average Center Frequencies f_c in GHz	Average Bandwidths B_j in GHz	Continuous Window Count
$\leq 0.3m$	424.5, 659.5, 842, 946	249, 173, 150, 50	4 ($\geq 50GHz$), 0 ($< 50GHz$)
$\leq 1m$	374.5, 498.5, 599, 684, 843, 946.5	149, 95, 44, 120, 146, 49	5 ($\geq 50GHz$), 1 ($< 50GHz$)
1 – 2m	340, 416.25, 497.25, 603.25, 683.25, 847, 946.5	80, 62.5, 88.5, 35.5, 114.5, 136, 43	5 ($\geq 50GHz$), 2 ($< 50GHz$)
3 – 10m	313, 351.7, 416.8, 466.7, 504.5, 611, 681.2, 854.7, 946.2	76.75, 56.75, 18.75, 56.5, 20, 104.5, 120.75, 36	5 ($\geq 50GHz$), 3 ($< 50GHz$)
10 – 11m	313, 351.5, 414.75, 467, 503.5, 611.5, 646.25, 694.25, 856.75, 945.75	26, 45, 46.5, 16, 48, 10, 25.5, 66.5, 106.5, 29.5	2 ($\geq 50GHz$), 8 ($< 50GHz$)

With the results shown in Fig. 2 we can infer that for a static model the δ_{min} values are highly dependent on the f_c , R_j and d_j values. In a static model, APs can be strategically placed to obtain higher throughput based on the frequency allocation available through regulators and environment impairments. For example, even with a small frequency window of $10GHz$ and a high Euclidian distance of $30m$, one can still obtain $10Gbps$ speed at a bare minimum beamwidth of 20° .

III. A MOBILITY MODEL

The analysis shown in Section 2 is true for static users and can be used to a certain extent by mobile users on a snapshot basis to select optimal frequency windows. However, when we add the impact of outages due to mobility of the users and orientation of the devices, the time-average throughput changes and so does the beamwidth values. The bare minimum beamwidth (shown in Fig. 2c and 2d) is not enough to maintain a time-average throughput as requested by the user. Before we estimate these optimal values, we need to identify these indoor small-scale mobility types.

In the future, indoor mobile THz devices will not only be limited to handheld displays, or Head Mounted Device (HMD) [12], but also augmented reality contact lenses, body area network (BAN), and nanobots. For lower beamwidths we need almost perfect alignment between the TX-RX antennas; thus, making these devices highly sensitive to fluctuations of hand, body, head (maybe even eye) movements. One of the highest throughput demanding use case for THz is VR & AR Games, which requires fast body and hand movements. Resulting in a user moving in all Six Degree of Freedom (DoF) as shown in the bottom right corner of Fig. 3. These games consist of bursts of high-intensity movements followed by slow movements, which can result in frequent misalignments. Although these VR games are sparsely used today, other applications such as VR chairs and VR goggles are gaining popularity among users

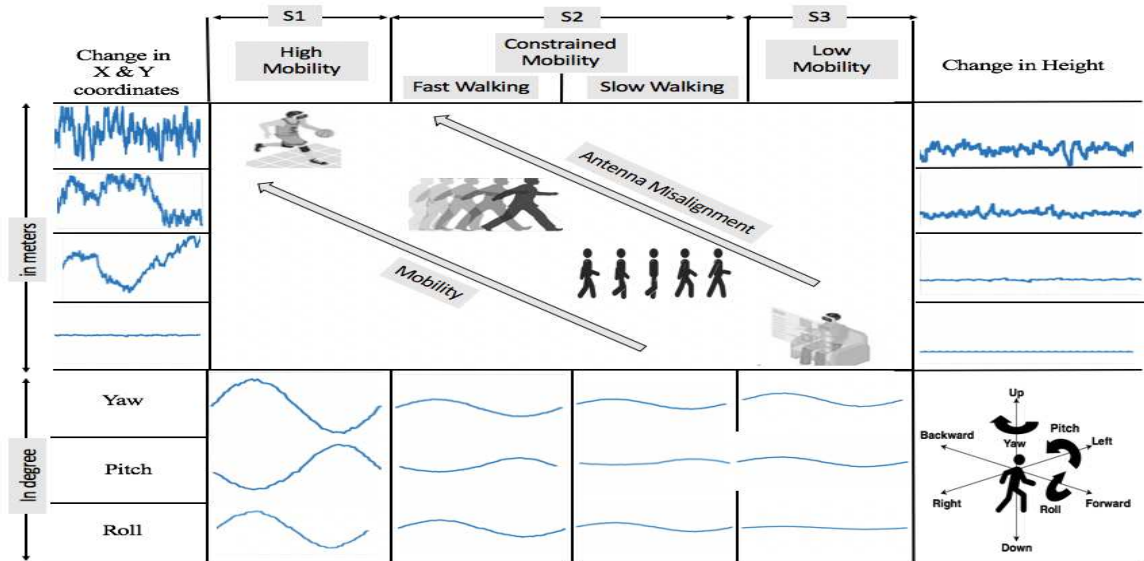


Fig. 3: Indoor Mobility Model showing the patterns associated with the Six-DoF of Human Body for different Action Types

to watch movies or play games. Compared to the action games, the body movements are relatively reduced in this scenario, yet these devices are still susceptible to misalignments due to yaw, pitch and roll motions of the body. A more constrained mobility scenario with low body fluctuations will be downloading or streaming uncompressed video while walking or standing in front of a kiosk or shared hotspot.

Whether it is a high-intensity game or even a constrained indoor mobility scenario, such as walking and standing, THz communication links, with narrow beamwidths, are susceptible to frequent misalignments. However, the best part of this movement is that they follow patterns. For example, in the case of action games, there are particular movements which are game specific and are repeated quite often, or in case of normal walking, the body repeats a particular velocity and movement pattern. In [15] it was shown that normal human walking is subjected to *bobbing*, i.e., the up and down movement of body's center of mass. The rate of bobbing is directly proportional to the velocity of the human. Thus, fast pace walking is more prone to misalignments than slow pace walking. Furthermore, while walking the yaw, pitch and roll motions of the body emulate a sinusoidal wave [16]. Even when a human is standing or in sedentary, it tends to move in small amounts in all the Six-DoF. The change in position while sedentary might look small but in scenarios with beamwidths less than (nearly) 5° can result in major misalignments. These features of human body movement can be parameterized for specific service types to provide the best QoS. Thus, there is a need to model these indoor mobility patterns using a set of parameters that can keep track of the Six-DoF. We name this parameter $\Theta = [\Delta x, \Delta y, \Delta z, \Delta \omega_y, \Delta \omega_p, \Delta \omega_r]$ as the *system instability parameter*, where the rate of change in x , y and z coordinates (*location parameters*) are represented by $\Delta x, \Delta y, \Delta z$ and change in yaw, pitch, and roll (*rotation parameters*) are represented by $\Delta \omega_y, \Delta \omega_p, \Delta \omega_r$.

Given the myriad number of multiple and small positional changes in the six dimensions of body movement, it is necessary that we have a model that imitates the human body based on service type. We bucket these activities into three major service type: (a) High Mobility (e.g., high intense games), (b) Constrained Mobility (e.g., fast and slow walking), and (c) Low Mobility (e.g., sitting or standing). A summary of the service types and the pattern of Θ values are shown in Fig. 3. Each service type is unique in both the mobility pattern and the demand for QoS. For service type S1 (High Mobility) there is random fluctuation in all six dimensions of the body. For service type S2 (Constrained Mobility) there is constant change in all six dimensions and is mostly proportional to the velocity of the body. We further divide the S2 into fast and slow walking. Since both fast and slow walking can cause bobbing, affecting the Δz and the rotation parameters, it is necessary that we monitor both of these cases separately in a constrained mobility scenario. For service type S3 (Low Mobility), it emulates more of a sedentary human, with very little change in the location parameters; yet, incorporates periodic oscillations in the rotational parameters. Detailed analysis shows that each of these parameters behaves in a particular pattern for a given type of movement. For example, research [16] on movement patterns of human walking showed sinusoidal yaw of the body with a peak amplitude of 4° . Moreover, the roll and pitch rotation also represented a sinusoidal wave, where the pitch amplitude decelerated and accelerated alternatively for each left and right roll movement of the body, as shown in Fig. 3. This shows that beamwidths narrower than body rotation may suffer from frequent misalignments if not monitored properly.

IV. OPTIMAL BEAMWIDTH FOR MOBILE USERS

For the simulations conducted in the rest of the paper, we assume a mobility that emulates Θ patterns mentioned in Fig. 3 and with values shown in Table II [15] [16] [17] [18]. Although the values in Table II are mostly dependent

TABLE II: User Mobility Parameters

Service Types	$\Delta x, \Delta y$	Δz	ω_y	ω_p	ω_r
S1	1 ± 0.5	0.5 ± 0.05	15.5°	13.8°	15°
S2	Fast Walk	0.9 ± 0.7	4°	5°	5°
	Slow Walk	0.3 ± 0.27	3°	3°	3°
S3	0 ± 0.01	0 ± 0.001	5°	3°	1°

on where the device is mounted (e.g., head, hand or eyes). For simplicity we consider the general body movement. This assumption is logically valid, since a human being's hand, head and body movements are somewhat interlinked. For example, if we move our hand to the left (or right) to grab an object our torso should also yaw in that direction.

We consider a room shown in Fig. 4 with M active users following a random way point model and requesting $10Gbps$ data rate per time slot. Each user can belong to either of the three service types shown in Fig. 3. Therefore, the instability parameter for a user j at any instance of time is defined as Θ_j^t , $t \in S1, S2, S3, j \in 1, 2, \dots, M$. For a fixed location of an AP (x_a, y_a, z_a) and a random user coordinates Θ_j^t , we can define d_j^t as the distance between the AP and UE j . To find a user's location, we use a random way point model coupled with the mean and standard division of the location parameters mentioned in Table II. Please note that to calculate the resultant z coordinate, we considered an average human standing height of $1.5m$ for S1 and S2, and a sitting height of $1.2m$ for S3. To calculate the rotational changes, we use the peak values of the rotation parameters mentioned in Table II to replicate sinusoidal wave patterns shown in Fig. 3. Please note that while a body is in motion, specifically in S1 and S2 scenarios, the pitch and roll movements experience alternative deceleration and acceleration, which is not present when a body is sedentary, i.e., in case of S3 [16]. We also allow the rotational movements through a small amount of noise to make the rotations more realistic. We assume the APs to be at three different locations, as shown in Fig. 4. Instead of a random AP placement, we explored 3 AP locations, Scenario A (middle of the ceiling), Scenario B (middle of the wall) and Scenario C (middle of the room on a $1m$ high table). As we move the AP away from one location in the room to another, the optimal beamwidth changes. Each AP location has its own advantages and disadvantages and is explained later.

It is obvious as the beamwidth increases the gain will decrease, eventually decreasing the throughput, as shown in Fig. 5. However, the AP placement also has a significant effect on the throughput. As we move from Scenario A to C, the throughput values increase rapidly, irrespective of the service types. Although Scenario A has a better coverage compared to Scenarios B and C, reducing the height of the antenna critically effects the system efficiency. Therefore, it will be beneficial to place the APs as close to the users as possible (due to high sensitivity to distance). For scenario A, all three service types have overlapping throughput values, and the gaps widen as we move to Scenarios B and C. Scenario B and C are effectively able to capture the yaw and pitch movements of the devices; thus, resulting in lower outages.

Although getting higher throughput is necessary, for a multi-

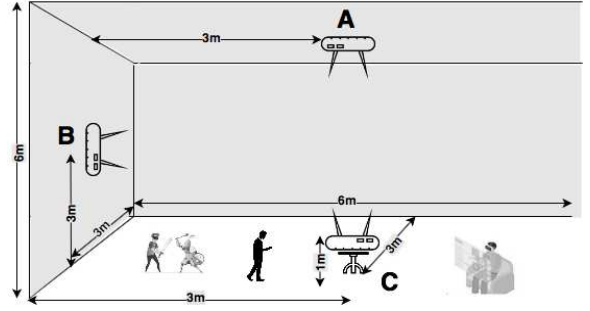


Fig. 4: Environment setting and different AP placement user scenario the critical system objective is to have a higher user coverage. For service type S2 and S3, Scenario B type AP placement shows on an average higher coverage compared to Scenario A and C, as shown in Fig. 6. While for Service type S1, on an average Scenario C shows higher coverage. We can even observe optimal beamwidth values for the different service types and AP placements. The nature of the curves is subjected to the human body movement as summarized in Fig. 3. If the rotation angle of the body (yaw, pitch, and roll) is higher than the beamwidth of the antenna, there are likely to be higher outages, resulting in a lower average user count. It is quite evident for S1, where the rotation angles are high and so are the outages are higher for very narrow beamwidths. On the contrary, S2 and S3 have relatively lower rotation angles, resulting in very low outages for lower beamwidth values.

The numerical evaluations are shown in Fig. 5 and 6 imply that for some fixed system parameters (frequency windows) there exists a δ_{opt} value that can help solve the “*beamwidth dilemma*” issue. There is a tradeoff between throughput and user-coverage based on: (a) device mobility parameter Θ^t , $t \in S1, S2, S3$, and (b) AP placement x_a, y_a, z_a . For example, to achieve higher user coverage for service type S1 users the $\delta_{opt} = 23^\circ$ for Scenario B, and $\delta_{opt} = 25^\circ$ for Scenario C. It seems for service type S2 and S3 type users the δ_{opt} values are lower, since with constrained and low mobility it is easier to satisfy multiple users at lower beamwidth values with minimum outages. It is harder to get higher coverage for S1 type users, due to the high fluctuation.

Although there are pros and cons to different AP placement type, each placement type can be used for different applications. Scenario A is likely to be in applications for VR games, office use or even in public safety events, where a drone (cluster head), out of a swarm of drones, can emulate a THz AP to get the maximum user coverage. On the other hand, Placement type B and C are more likely for applications for indoor users, ultra-high-speed kiosks or used as personal hotspots at waiting lounges. The analysis supports the need for adaptively changing beamwidths (and other system parameters) based on service type and antenna placement.

V. CONCLUSION

In this paper, we analyze parameters, such as frequency, beamwidth, AP placement, and mobility type that are necessary for higher throughput and user coverage for indoor THz communications. To use THz resource more economically

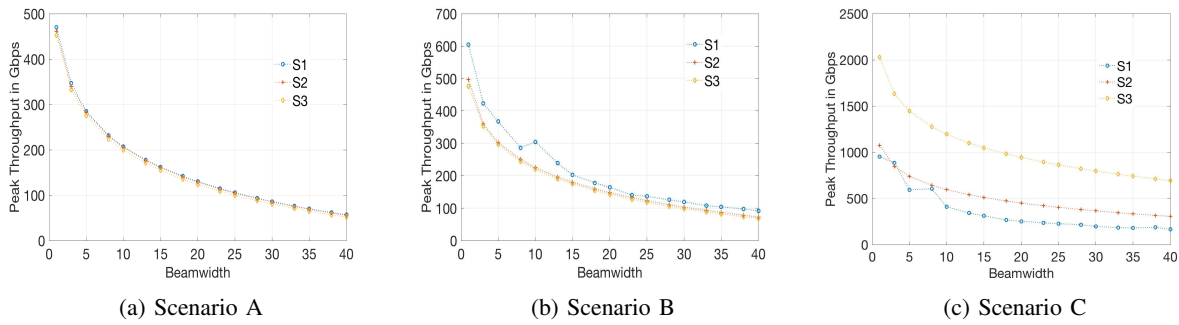


Fig. 5: Peak Throughput for different service types and AP placements

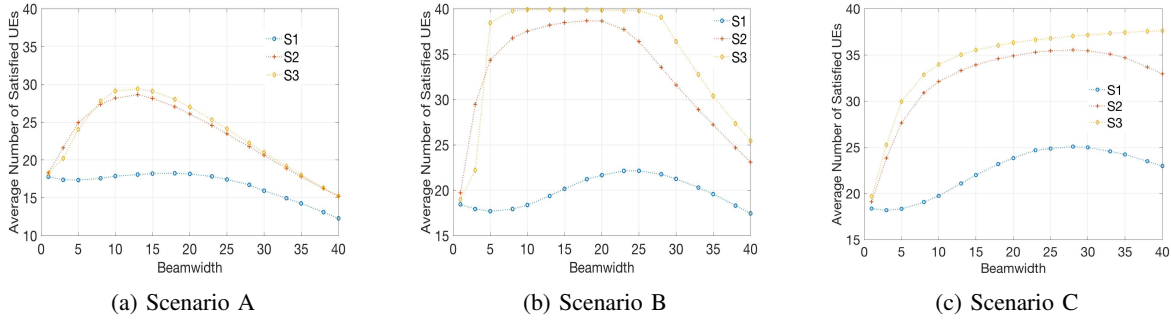


Fig. 6: Average User Coverage for different service types and AP placements

and opportunistically, we (a) perform numerical analysis for a single AP, (b) characterize the small-scale mobility type based on the human actions, and (c) quantify the relationship between beamwidth and other system parameters. We observe that for static applications a theoretical bound for the beamwidth can be drawn based on the system parameters such as frequency and requested data rate. While for the mobile applications, we observe that the services type and the nature of the device orientation can significantly affect the optimal beamwidth. In a mobile scenario, the optimal beamwidths are not only dependent on service type, but also the AP location. Our parameter analysis for static and mobile applications will help address issues related to THz deployment (frequency and AP placement) and “*beamwidth dilemma*” for indoor settings. Systems can dynamically change the δ_{opt} values based on four critical factors: (a) objective functions (throughput or user coverage), (b) frequency windows, (c) mobility parameters Θ^t , and (d) AP locations.

REFERENCES

- [1] E. C. Strinati, et.al., “6G: The Next Frontier,” Jan 2019. Available: <https://arxiv.org/abs/1901.03239>
- [2] A. Ghosh, et.al., “Millimeter-Wave Enhanced Local Area Systems: A High-Data-Rate Approach for Future Wireless Networks,” *IEEE Journal on Selected Areas in Communications*, vol. 32, no. 6, pp. 1152-1163, June 2014.
- [3] Y. Ghasempour, C. R. C. M. da Silva, C. Cordeiro, E. W. Knightly, “IEEE 802.11ay: Next-Generation 60 GHz Communication for 100 Gb/s Wi-Fi,” *IEEE Communications Magazine*, vol. 55, no. 12, pp. 186-192, Dec 2017.
- [4] Radiocommunication Sector of International Telecommunication Union (ITU), “Attenuation by atmospheric gases-P Series Radiowave propagation,” Tech.Rep. ITU-R P.676-10, 2013.
- [5] I. F. Akyildiz, J. M. Jornet, C. Han, “TeraNets: ultra-broadband communication networks in the terahertz band,” *IEEE Wireless Communications*, vol. 21, no. 4, pp. 130-135, Aug 2014.
- [6] A. A. Boulogeorgos ; E. N. Papatotiriou; A. Alexiou, “A Distance and Bandwidth Dependent Adaptive Modulation Scheme for THz Communications,” in *Proc. of IEEE 19th International Workshop on Signal Processing Advances in Wireless Communications (SPAWC)*, Jun. 2018.
- [7] C. Han, A. O. Bicen, I. F. Akyildiz, “Multi-Ray Channel Modeling and Wideband Characterization for Wireless Communications in the Terahertz Band,” *IEEE Transactions on Wireless Communications*, vol. 14, no. 5, pp. 2402 - 2412, May 2015.
- [8] Q. Z. Sai, H.T. Kung, Y. Gwon, “InferBeam: A Fast Beam Alignment Protocol for Millimeter-wave Networking,” [online] Available: <https://arxiv.org/pdf/1802.03373.pdf>.
- [9] C. Lin, G. Y. Li, “Indoor Terahertz Communications: How Many Antenna Arrays Are Needed?,” *IEEE Transactions on Wireless Communications*, vol. 14, no. 6, pp. 3097-3107, Jun 2015.
- [10] T. Schneider, et.al., “Link Budget Analysis for Terahertz Fixed Wireless Links,” *IEEE Transactions on Terahertz Science and Technology*, vol. 2, no. 2, pp. 250-256, 2012.
- [11] V. Petrov, D. Moltchanov, Y. Koucheryavy, J. M. Jornet, “The effect of small-scale mobility on terahertz band communications,” in *Proc. of the 5th ACM International Conference on Nanoscale Computing and Communication (NANOCOM)*, no. 40, Sept. 2018.
- [12] R. Azuma, et.al., “Recent advances in augmented reality,” *IEEE Computer Graphics and Applications*, vol. 21, no. 6, pp. 34-47, 2001.
- [13] R. Singh, S. Mukherjee, S. C. Ghosh, “Improving User Coverage Through Resource Aware Handoff Management in Heterogeneous Networks,” in *Proc. 13th International Conference on Advances in Mobile Computing and Multimedia (MoMM)*, Dec. 2015, pp. 179-188.
- [14] J. E. Hill, “Gain of Directional Antennas,” Watkins-Johnson Company Tech-notes, 1976. Tech.Rep.
- [15] F. Massaad, T. M. Lejeune, C. Detrembleur, “The up and down bobbing of human walking: a compromise between muscle work and efficiency,” *J. Physiol.*, vol. 582, no. 2, pp. 789-799, 2007.
- [16] T. Imai, S. T. Moore, T. Raphan, B. Cohen, “Interaction of the body, head, and eyes during walking and turning,” *Exp Brain Res, Springer*, vol. 136, no. 1, pp. 1-18, 2001.
- [17] T. Otani, et.al, “Upper-Body Control and Mechanism of Humanoids to Compensate for Angular Momentum in the Yaw Direction Based on Human Running,” in *Proc. IEEE International Conference on Robotics and Automation (ICRA)*, 2017.
- [18] D.C. Niehorster, L. Li, M. Lappe, “The Accuracy and Precision of Position and Orientation Tracking in the HTC Vive Virtual Reality System for Scientific Research,” *Iperception*, vol. 8, no. 3, 2017.